arXiv:0808.1952v1 [cond-mat.stat-mech] 14 Aug 2008

Correlation of spin and velocity in granular gases

W. T. Kranz,[1] N. V. Brilliantov,[2] T. Pöschel,[3] and A. Zippelius[1, 4]
[1]*Max Planck Institute for Dynamics and Self Organization, Bunsenstr. 10, 37073 Göttingen, Germany*
[2]*Department of Mathematics, University of Leicester, University Road, Leicester LE1 7RH UK*
[3]*Universität Bayreuth, Physikalisches Institut, 95440 Bayreuth, Germany*
[4]*Institute of Theoretical Physics, University of Göttingen, Friedrich-Hund-Platz 1, 37077 Göttingen*

(Dated: August 14, 2008)

In a granular gas of rough particles the spin of a grain is correlated with its linear velocity. We develop an analytical theory to account for these correlations and compare its predictions to numerical simulations, using Direct Simulation Monte Carlo as well as Molecular Dynamics. The system is shown to relax from an arbitrary initial state to a quasi-stationary state, which is characterized by time-independent, finite correlations of spin and linear velocity. The latter are analysed systematically for a wide range of system parameters, including the coefficients of tangential and normal restitution as well as the moment of inertia of the particles. For most parameter values the axis of rotation and the direction of linear momentum are perpendicular like in a sliced tennis ball, while parallel orientation, like in a rifled bullet, occurs only for a small range of parameters. The limit of smooth spheres is singular: any arbitrarily small roughness unavoidably causes significant translation-rotation correlations, whereas for perfectly smooth spheres the rotational degrees of freedom are completely decoupled from the dynamic evolution of the gas.

PACS numbers: 45.70.-n, 45.70.Qj, 47.20.-k

I. INTRODUCTION

Materials which are composed of macroscopic objects, i.e. granular media, attract increasing scientific interest due to their importance in nature and technology, e.g. [1, 2]. The latter may be exemplified by transport and storage of sand, cereals, granular chemicals, etc. the former–by avalanches, land slides, dust devils, etc. Spectacular celestial objects, like planetary rings or interstellar dust clouds, can serve as another example of natural granular systems [3]. The granular matter exists there in a gaseous state and exhibits many properties of a common molecular gas, e.g. [1, 4, 5, 6]. The main (and very important) difference of a granular gas from a molecular gas is the *dissipative* nature of particle interactions, which are describe by macroscopic mechanics of solids rather than by a microscopic interaction potential. The consequences of the dissipative interactions are quite substantial: A spatially homogeneous state is unstable [7, 8, 9], velocities are not distributed according to a Maxwell-Boltzmann distribution [10, 11, 12, 13, 14, 15, 16, 17, 18] and the diffusion or self-diffusion is anomalous [19, 20, 21, 22, 23]. These properties of a granular gas have been observed for the case of smooth particles, when grain collisions do not affect their rotational motion. This is, certainly, an oversimplified model, since real grains have a rough surface and exchange rotational and translational energy in collisions.

Real granular particles experience *frictional forces* when colliding. Hence, a more adequate model takes into account the rotational motion of particles and the exchange of rotational and translational energy in collisions [1, 6, 10, 24, 25, 26, 27, 28, 29, 30, 31, 32, 33, 34, 35]. Dissipative frictional gases exhibit additional unusual features which are not present in molecular gases. For instance, equipartition between rotational and translational motion does not hold [24] and the hydrodynamic description requires an additional field and a dynamic equation to account for its evolution [26, 36]. Moreover, the rotational and translational motion of particles are correlated as mentioned in a very implicit way in Appendix E of [26] and worked out in [37]. In the present study we analyze the latter effect in detail.

In Sec II we introduce a model of frictional particles and the observables of interest. Subsequently in Sec. III an approximate analytical theory is developed and in Sec. IV we briefly explain the simulation techniques. The main results are presented in Sec. V, where we compare predictions of the analytical theory with data from simulations. The emphasis lies on the correlations in the quasi-steady state, but we also briefly discuss the relaxation to the steady state. The technical details of the calculations are given in the Appendix.

II. MODEL AND OBSERVABLES

We consider a granular gas consisting of N inelastic hard spheres of radius a, mass m, and moment of inertia $I = qma^2$. Here the dimensionless variable q is determined by the mass distribution within the disc. The state of the system is fully described by the particles' positions $\{\boldsymbol{r}_i\}$, velocities $\{\boldsymbol{v}_i\}$, and angular velocities $\{\boldsymbol{\omega}_i\}$ for $i = 1, \ldots, N$. The particles move freely in between *instantaneous* collisions, whereupon their linear and angular velocities change according to the collision rule: the relative velocity at the point of contact of colliding particles is

$$\boldsymbol{g} \equiv \boldsymbol{v}_1 - \boldsymbol{v}_2 + a\hat{\boldsymbol{n}} \times (\boldsymbol{\omega}_1 + \boldsymbol{\omega}_2)\,, \tag{1}$$

with $\hat{\boldsymbol{n}} \equiv \hat{\boldsymbol{n}}_{12} \equiv (\boldsymbol{r}_1 - \boldsymbol{r}_2) / |\boldsymbol{r}_1 - \boldsymbol{r}_2|$. The post-collisional (primed) velocity is related to the pre-collisional one by

$$\begin{aligned} \boldsymbol{g}' \cdot \hat{\boldsymbol{n}} &= -\varepsilon_n \, \boldsymbol{g} \cdot \hat{\boldsymbol{n}} \\ \boldsymbol{g}' \times \hat{\boldsymbol{n}} &= \varepsilon_t \, \boldsymbol{g} \times \hat{\boldsymbol{n}} \,. \end{aligned} \tag{2}$$

The coefficient of normal restitution is denoted by ε_n with $0 \leq \varepsilon_n \leq 1$. The value $\varepsilon_n = 0$ implies no relative motion in the normal direction after the collision, whereas for $\varepsilon_n = 1$ no dissipation of the normal component of the relative motion occurs. The coefficient of tangential restitution has two elastic limits, namely $\varepsilon_t = 1$ corresponding to smooth spheres and $\varepsilon_t = -1$ corresponding to perfectly rough (reflecting) collisions without loss of energy for the tangential motion. For all other values energy is lost in the tangential component. In general, both coefficients of restitution, ε_n and ε_t, depend on the impact velocity [38, 39, 40, 41].

Together with the conservation of linear and angular momentum the collision rule, Eq. (2), determines the post-collisional velocities in terms of the pre-collisional ones:

$$\begin{aligned} \boldsymbol{v}_1' &= \boldsymbol{v}_1 - \boldsymbol{\delta}, \quad \boldsymbol{\omega}_1' = \boldsymbol{\omega}_1 + \frac{1}{qa}(\hat{\boldsymbol{n}} \times \boldsymbol{\delta}) \\ \boldsymbol{v}_2' &= \boldsymbol{v}_2 + \boldsymbol{\delta}, \quad \boldsymbol{\omega}_2' = \boldsymbol{\omega}_2 + \frac{1}{qa}(\hat{\boldsymbol{n}} \times \boldsymbol{\delta}) \,, \end{aligned} \tag{3}$$

where $m\boldsymbol{\delta}$ denotes the exchange of linear momentum with

$$\boldsymbol{\delta} \equiv \eta_t \boldsymbol{g} + (\eta_n - \eta_t)(\hat{\boldsymbol{n}} \cdot \boldsymbol{g})\hat{\boldsymbol{n}} \,, \tag{4}$$

$$\eta_n \equiv \frac{1+\varepsilon_n}{2} \,, \qquad \eta_t \equiv \frac{q}{2}\, \frac{1-\varepsilon_t}{1+q} \,. \tag{5}$$

In the present study we address only non-driven systems. Moreover, we focus on the homogeneous cooling state (HCS) of a gas, which is characterized by two time-dependent granular temperatures, one for the translational and one for the rotational motion,

$$T = \frac{m}{3N} \sum_{i=1}^{N} \boldsymbol{v}_i^2 \quad \text{and} \quad R = \frac{I}{3N} \sum_{i=1}^{N} \boldsymbol{\omega}_i^2. \tag{6}$$

One generally observes that after a transient period the system reaches a quasi-stationary state where $r \equiv R(t)/T(t) = \text{const.}$, that is, both temperatures decay with the same rate. In general, $r \neq 1$ so that equipartition is violated. The value of r depends on the collision parameters as well as on the moment of inertia [24, 42].

In this paper we focus on the correlation between the axis of rotation of a granular particle and the direction of its linear velocity, which may be quantified by the angle θ_i between the linear and rotational velocity,

$$\cos\theta_i = \frac{\boldsymbol{v}_i \cdot \boldsymbol{\omega}_i}{|\boldsymbol{v}_i||\boldsymbol{\omega}_i|}. \tag{7}$$

All information on the angle is contained in the distribution

$$f(\cos\theta) = \frac{1}{N} \sum_{i=1}^{N} \delta(\cos\theta - \cos\theta_i), \tag{8}$$

In a molecular gas all values of $\cos\theta$ occur with equal probability due to equipartition. In contrast for a granular gas we know that equipartition is violated and we expect to observe deviations from the equi-distribution.

Because of symmetry, the average of $\cos\theta_i$ over all particles vanishes. Thus, a measure of correlations is the second moment,

$$\left\langle \cos^2\theta \right\rangle = \frac{1}{N} \sum_i \frac{(\boldsymbol{v}_i \cdot \boldsymbol{\omega}_i)^2}{\boldsymbol{v}_i^2 \boldsymbol{\omega}_i^2} \,. \tag{9}$$

If the angular and linear velocities are not correlated in their direction, $\left\langle \cos^2\theta \right\rangle = 1/3$. Hence, any deviation of $\left\langle \cos^2\theta \right\rangle$ from $1/3$ indicates correlations. Moreover, if $\left\langle \cos^2\theta \right\rangle < 1/3$ the angular and linear velocities are preferably perpendicular, like in a sliced tennis ball, while for $\left\langle \cos^2\theta \right\rangle > 1/3$ they are preferably aligned like in a rifled bullet.

III. ANALYTICAL THEORY

The evolution of any observable

$$F(t) = F\left(\{\boldsymbol{r}_i(t), \boldsymbol{v}_i(t), \boldsymbol{\omega}_i(t)\}\right) \tag{10}$$

may be obtained by means of the pseudo-Liouville operator $\mathcal{L}_+$ via

$$\partial_t F(t) = i\mathcal{L}_+ F(t) \quad \text{for} \quad t > 0. \tag{11}$$

For hard spheres the pseudo-Liouville operator decomposes into two parts, $\mathcal{L}_+ = \mathcal{L}_0 + \mathcal{L}_+'$, where $\mathcal{L}_0 = \mathcal{L}_0^{\text{tr}} + \mathcal{L}_0^{\text{rot}}$ describes the free streaming of translational and rotational motion of particles. Here $\mathcal{L}_0^{\text{tr}} = \sum_i \boldsymbol{v}_i \cdot \nabla_i$ and a similar expression for $\mathcal{L}_0^{\text{rot}}$. The latter is not needed here, because we never specify the orientation of our particles , which are perfect spheres. The interaction part of the pseudo-Liouville operator reads, $\mathcal{L}_+' = \sum_{i<j} \mathcal{T}_{ij}$, where the binary collision operator $\mathcal{T}_{ij}$ reads [11, 24]

$$i\mathcal{T}_{ij} = -\hat{\boldsymbol{n}}_{ij} \cdot \boldsymbol{v}_{ij} \Theta\left(-\hat{\boldsymbol{n}}_{ij} \cdot \boldsymbol{v}_{ij}\right) \delta\left(r_{ij} - 2a\right) \left(\hat{b}_{ij} - 1\right) . \tag{12}$$

The operator $\hat{b}_{ij}$ replaces unprimed by primed values according to the collision rule, Eq. (3). For example,

$$\hat{b}_{12}\boldsymbol{v}_1 = \boldsymbol{v}_1' \,, \qquad \hat{b}_{12}\boldsymbol{v}_2 = \boldsymbol{v}_2' \,, \qquad \hat{b}_{12}\boldsymbol{v}_k = \boldsymbol{v}_k \,, \quad k \neq 1, 2 \tag{13}$$

with $\boldsymbol{v}_1'$ and $\boldsymbol{v}_2'$ given by Eq. (3) and with similar relations for the rotational velocities.

The ensemble average of a dynamic variable is defined by

$$\langle F \rangle_t = \int d\Gamma \rho(0) F(t) = \int d\Gamma \rho(t) F(0) \tag{14}$$

with $d\Gamma = \prod_i (d^3 r_i d^3 v_i d^3 \omega_i)$. Here $F(t) = \exp(-i\mathcal{L}_+ t) F(0)$ and $\rho(t) = \exp(-i\mathcal{L}_+^\dagger t)\rho(0)$ denotes the N-particle distribution, whose evolution is governed by the adjoint $\mathcal{L}_+^\dagger$ of the evolution operator $\mathcal{L}_+$. Differentiating Eq. (14) one obtains

$$\begin{aligned} \frac{d}{dt}\left\langle F \right\rangle_t &= \int d\Gamma \rho(0) \frac{d}{dt} F(t) = \int d\Gamma \rho(0) i\mathcal{L}_+ F(t) \\ &= \int d\Gamma \rho(0) \exp(i\mathcal{L}_+ t) i\mathcal{L}_+ F(0) \\ &= \int d\Gamma \rho(t) i\mathcal{L}_+ F(0) = \left\langle i\mathcal{L}_+ F \right\rangle_t . \end{aligned} \tag{15}$$

It is impossible to compute the time-dependent N-particle distribution exactly, so that we have to resort to approximations. A standard procedure in the analytical treatment of granular gases is to assume homogeneity and molecular chaos, e.g. [6] (see also [43]). Under these assumptions the N-particle velocity distribution function takes the form

$$\rho(t) = g_N(\boldsymbol{r}_1, \ldots, \boldsymbol{r}_N) \prod_i \rho_1(\boldsymbol{v}_i, \boldsymbol{\omega}_i, t), \tag{16}$$

where the N-particle correlation function of a hard sphere system, $g_N(\boldsymbol{r}_1, \ldots, \boldsymbol{r}_N)$, is not affected by the particle roughness. For the HCS it may be approximated by the corresponding function of an equilibrium hard-sphere system (e.g. [6]). For an isotropic system $\rho_1(\boldsymbol{v}, \boldsymbol{\omega})$ depends in general on $v = |\boldsymbol{v}|, \omega = |\boldsymbol{\omega}|$ and the angle θ ($\cos\theta = \boldsymbol{v} \cdot \boldsymbol{\omega} / (|\boldsymbol{v}|\,|\boldsymbol{\omega}|)$. Here we are particularly interested in the dependence on $\cos\theta$ and expand ρ_1 in Legendre polynomials $P_n(\cos\theta)$

$$\begin{aligned} \rho_1(\boldsymbol{v}, \boldsymbol{\omega}, t) \propto & \exp\left(-\frac{m\boldsymbol{v}^2}{2T(t)}\right) \exp\left(-\frac{I\boldsymbol{\omega}^2}{2R(t)}\right) \\ & \times \sum_{n=0}^{\infty} b_n(t) \boldsymbol{v}^n \boldsymbol{\omega}^n P_n(\cos\theta), \end{aligned} \tag{17}$$

where the $b_n(t)$ are time dependent expansion coefficients and the distribution function has to be normalized according to $\int d\Gamma \rho_1 = 1$. We use a simple Gaussian even though the distributions are non-Gaussian for strong dissipation and high densities. Deviations have been handled by an expansion in Sonine polynomials [44]. Here we concentrate on the dependence on $\cos\theta$ and leave a more general ansatz with both, angular correlations and non-Gaussian distributions, to future work. To keep the calculations tractable, we limit the calculation to the lowest non-trivial order

$$\begin{aligned} \rho_1(\boldsymbol{v}, \boldsymbol{\omega}, t) \propto & \exp\left(-\frac{m\boldsymbol{v}^2}{2T(t)}\right) \exp\left(-\frac{I\boldsymbol{\omega}^2}{2R(t)}\right) \\ & \times \left[1 + b(t) \boldsymbol{v}^2 \boldsymbol{\omega}^2 P_2(\cos\theta)\right], \end{aligned} \tag{18}$$

where $b(t) \equiv b_2(t)$ and $P_2(\cos\theta) = {}^3\!/_2(\cos^2\theta - {}^1\!/_3)$. The terms for odd n vanish by symmetry.

The lowest order coefficient $b(t)$ is simply related to the quantity of interest $\left\langle \cos^2\theta \right\rangle_t$. Using $P_0(\cos\theta) = 1$ and expressing $\left\langle \cos^2\theta \right\rangle_t$ in terms of Legendre polynomials we can write

$$\begin{aligned} \left\langle \cos^2\theta \right\rangle_t = \frac{1}{3} \int_v \int_\omega & [P_0(\cos\theta) + 2P_2(\cos\theta)] \\ & \times [P_0(\cos\theta) + b(t) v^2 \omega^2 P_2(\cos\theta)] \end{aligned} \tag{19}$$

where for brevity we introduce the shorthand notation

$$\int_v = \left(\frac{m}{2\pi T}\right)^{3/2} \int d^3 v \, \exp\left(-\frac{mv^2}{2T}\right) \tag{20}$$

and similarly for $\int_\omega$. The angular integration in the Eq. (19) may be performed using the orthogonality relation for Legendre polynomials, yielding

$$\left\langle \cos^2\theta \right\rangle_t = \frac{1}{3} + b(t) \frac{6T(t)R(t)}{5qm^2a^2}. \tag{21}$$

Hence, the correlations of interest manifest themselves through the coefficient $b(t)$–the larger the coefficient, the more pronounced are deviations from the value $\left\langle \cos^2\theta \right\rangle = 1/3$ of the uncorrelated case.

To summarize our analytical approach so far: The time dependent N-particle distribution has been parametrised by three time-dependent functions $T(t)$, $R(t)$ and $b(t)$, which have to be calculated self-consistently. This is achieved by applying the general equation (15) for the evolution of an observable to $T(t)$, $R(t)$ and $b(t)$ and using our ansatz for $\rho(t)$, see Eqs. (16,18). Even with all these simplifying assumptions, the analytical calculations are rather cumbersome and all the details of the calculation have been relegated to the Appendix.

The results are three first order differential equations for $T(t), R(t)$ and $b(t)$. These simplify, if we measure times in units of the Enskog collision frequency $\omega_E = 16(\pi T/m)^{1/2} n a^2 g_2(2a)$. In other words we rescale time according to $d\tau = \omega_E dt$ and obtain:

$$\begin{aligned} \frac{dT}{d\tau} &= -AT(\tau) + B\left[1 - \frac{b(\tau)}{2}\frac{T(\tau)R(\tau)}{qm^2a^2}\right] R(\tau) \\ \frac{dR}{d\tau} &= BT(\tau) - C\left[1 - \frac{b(\tau)}{2}\frac{T(\tau)R(\tau)}{qm^2a^2}\right] R(\tau) \end{aligned} \tag{22}$$

where

$$\begin{aligned} & A \equiv \eta_n(1-\eta_n) + \eta_t(1-\eta_t), \\ & B \equiv \frac{\eta_t^2}{q}, \qquad C \equiv \frac{\eta_t}{q}\left(1 - \frac{\eta_t}{q}\right). \end{aligned} \tag{23}$$

and

$$\begin{aligned} 20\frac{db}{d\tau} = & -b(\tau)\left[A^{(1)} + B^{(1)}\frac{R(\tau)}{T(\tau)} + \frac{40}{T(\tau)}\frac{dT}{d\tau}(\tau) \right. \\ & \left. + \frac{40}{R(\tau)}\frac{dR}{d\tau}(\tau)\right] \\ & - \frac{qm^2a^2}{T(\tau)R(\tau)}\left[A^{(0)} + B^{(0)}\frac{R(\tau)}{T(\tau)} + C^{(0)}\frac{T(\tau)}{R(\tau)}\right]. \end{aligned} \tag{24}$$

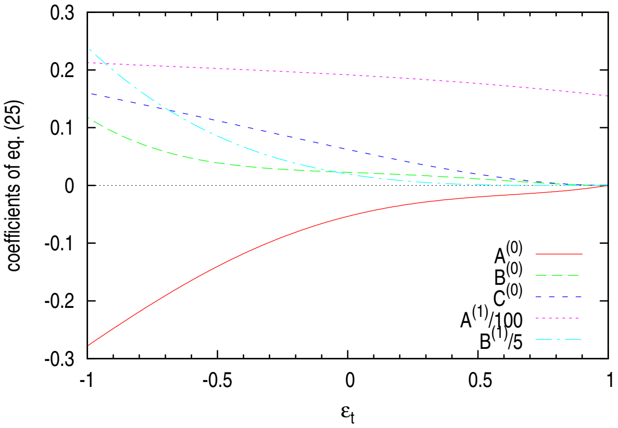

FIG. 1: (Color online) The coefficients in Eq. (25) as a function of ε_t for $\varepsilon_n = 0.9$ and $q = 2/5$. Note that $B^{(1)}$ is slightly negative for $\varepsilon_t \gtrsim 0.7$. Except for the coefficient $A^{(0)}$ all coefficients vanish in the limit $\varepsilon_t \to 1$.

The constants are given by:

$$A^{(0)} \equiv \frac{16}{3}\frac{\eta_t^3}{q}\left(\frac{2\eta_t}{q}-1\right) - \frac{2}{3}\frac{\eta_t^2}{q}\left(\frac{8\eta_t}{q}-3\right) + \frac{1}{3}\frac{\eta_t}{q}\left(\frac{\eta_t}{q}-1\right) + \frac{8}{3}\frac{\eta_t}{q}\left(\frac{\eta_t}{q}-1\right)\eta_n(\eta_n-1) \tag{25a}$$

$$B^{(0)} \equiv \frac{1}{3}\frac{\eta_t^2}{q}\left[\frac{16\eta_t}{q}\left(\frac{\eta_t}{q}-1\right)+5\right] \tag{25b}$$

$$C^{(0)} \equiv \frac{2}{3}\frac{\eta_t^2}{q}\left[8\eta_t(\eta_t-1)+4\eta_n(\eta_n-1)+3\right] \tag{25c}$$

$$A^{(1)} \equiv -\frac{8\eta_t^3}{q}\left(\frac{2\eta_t}{q}-1\right) + \frac{1}{3}\frac{\eta_t^2}{q}\left(\frac{24\eta_t}{q}-37\right) - \frac{5}{6}\frac{\eta_t}{q}\left(\frac{9\eta_t}{q}-29\right) - \frac{4\eta_t\eta_n^2}{q}\left(\frac{\eta_t}{q}-1\right) + \frac{4}{3}\frac{\eta_t\eta_n}{q}\left(\frac{3\eta_t}{q}-14\right) - 12\eta_t\eta_n + 22(\eta_t+\eta_n) - 6(\eta_t^2+\eta_n^2) \tag{25d}$$

$$B^{(1)} \equiv -\frac{2}{3}\frac{\eta_t^2}{q}\left[\frac{8\eta_t}{q}\left(\frac{\eta_t}{q}-1\right)+1\right]. \tag{25e}$$

Eqs. (22) and (24) constitute a set of self-consistent equations for the observables $T(t), R(t)$, and $b(t)$. Fig. 1 illustrates the dependence of the above coefficients on the coefficient of tangential restitution.

IV. SIMULATIONS

We performed both Direct Simulation Monte Carlo (DSMC) [45] and event-driven Molecular Dynamics (MD) [46] calculations to check the predictions of the analytical theory. DSMC determines the stationary distribution of the scaled velocities by numerically solving the kinetic Boltzmann equation which is based on the assumption of molecular chaos. Consequently, for its application it is assumed that the gas is uniform, thus, spatial correlations of the particles are neglected. If this precondition is given, DSMC yields very precise statistical results because of the large number of particles which can be simulated (here we use $N = 2 \times 10^7$ particles[49]).

Molecular Dynamics calculates the trajectories of the particles using the collision rule, Eq. (2), therefore, MD allows to trace the evolution of the correlation. On the other hand, MD is restricted to much smaller systems as compared to DSMC. Although MD is free from the mentioned assumptions, DSMC is significantly more efficient for a homogeneous granular gas. Moreover, in the limit of low density both methods provide, in principle, identical results for the stationary state [46]. In practice, we use MD for $N = 8000$ particles to study the transient process of the system's relaxation to its steady-state and up to $N = 10^5$ for steady state correlations. The volume fraction is $\frac{N}{V}\frac{4\pi a^3}{3} = 0.0146$ or even smaller, such that the gas is always in the HCS.

V. RESULTS

Starting from a random distribution of velocities and angular velocities with mean $\langle \boldsymbol{v} \rangle = \langle \omega \rangle = 0$, after some transient period the system relaxes to a steady state where the correlation of the spin and the translational velocity as well as the ratio of translational and rotational temperatures adopt stationary values. We quantify these correlations by means of the second moment $\left\langle \cos^2\theta \right\rangle$, see Eq. (9) and analyze this quantity as a function of three parameters, ε_n, ε_t, and q in Sec. V A. The relaxation to the steady state is discussed in Sec. V B and in Sec. V C we consider correlations beyond the second moment and investigate the distribution of $\cos\theta$.

A. Steady-state correlations

To study the steady-state properties it is convenient to introduce an auxiliary variable

$$x(\tau) \equiv b(\tau)\frac{T(\tau)R(\tau)}{qm^2a^2} = \frac{5}{6}\left(\left\langle \cos^2\theta \right\rangle_\tau - \frac{1}{3}\right). \tag{26}$$

Using $x(\tau)$ and $r(\tau) = R(\tau)/T(\tau)$ we recast the set of three equations (22,24) for b, R and T into a set of two equations for x and r. The result reads

$$
\begin{aligned}
\frac{dr}{d\tau} &= B - C\left[1 - \frac{x(\tau)}{2}\right] r(\tau) + A r(\tau) - B\left[1 - \frac{x(\tau)}{2}\right] r^2(\tau) && (27)\\
20\frac{dx}{d\tau} &= -x(\tau)\left\{A^{(1)} + B^{(1)} r(\tau) - 20A - 20C + 20B[r(\tau) + r^{-1}(\tau)] + 20x(\tau)[C - B\, r(\tau)]/2\right\} && (28)\\
&- A^{(0)} - B^{(0)} r(\tau) - C^{(0)} r^{-1}(\tau)\,.
\end{aligned}
$$

Setting the left hand side of Eqs. (27) and (28) to zero one arrives at a set of coupled nonlinear equations for the stationary values $r_\infty \equiv r(\tau \to \infty)$ and $x_\infty \equiv x(\tau \to \infty)$. Instead of solving these equations directly, we resort to an iteration scheme: At the outset we calculate a first approximation of the temperature ratio $r_\infty^{(0)}$ neglecting correlations, that is, for $x = 0$. Hence we assume that for moderate inelasticity and roughness the temperature ratio is not noticeably affected by the rotational-translational coupling. The result reads

$$
r_\infty^{(0)} = \frac{A - C}{2B} + \sqrt{1 + \frac{(A - C)^2}{4B^2}}\,. \qquad (29)
$$

Using this value for the stationary temperature ratio we then proceed to calculate an approximate value of x_∞

$$
x_\infty^{(0)} = -\frac{A^{(0)} + B^{(0)} r_\infty^{(0)} + C^{(0)}/r_\infty^{(0)}}{A^{(1)} + B^{(1)} r_\infty^{(0)} - 40C + 40B/r_\infty^{(0)}} \qquad (30)
$$

where we use the fact, that

$$
B\left[r_\infty^{(0)} + 1/r_\infty^{(0)}\right] = A - C + 2B/r_\infty^{(0)} \qquad (31)
$$

and neglect the terms quadratic in x_∞ since they are presumably small. In principle, one could further iterate to get better approximations, but we find that the results are reasonably good already at this stage. For the more intuitive variable, $\cos^2\theta$, Eq. (30) implies

$$
\left\langle \cos^2\theta \right\rangle_\infty \approx \frac{1}{3} - \frac{6}{5}\,\frac{A^{(0)} + B^{(0)} r_\infty^{(0)} + C^{(0)}/r_\infty^{(0)}}{A^{(1)} + B^{(1)} r_\infty^{(0)} + 40B/r_\infty^{(0)} - 40C}\,. \qquad (32)
$$

Fig. 2 shows the steady-state value of the correlation factor $\left\langle \cos^2\theta \right\rangle_\infty$ as a function of ε_t for different values of ε_n in comparison with DSMC results. Obviously, theory as well as simulations show that both types of correlations may occur, $\left\langle \cos^2\theta \right\rangle < 1/3$, as for a sliced tennis ball or $\left\langle \cos^2\theta \right\rangle > 1/3$ as for a rifled bullet The dependence of the correlations on ε_t is nonmonotonic with the strongest correlations for $\varepsilon_t \sim 0$ and $\varepsilon_t \to 1$. Even though the dependence on ε_n is also not strictly monotonic, the dominant tendency is an increase of correlations with decreasing ε_n, i.e. increasing inelasticity. The agreement between theory and computer experiment is excellent for small inelasticity. Moreover, even for significant dissipation the theory is able to reproduce qualitatively the simulation results.

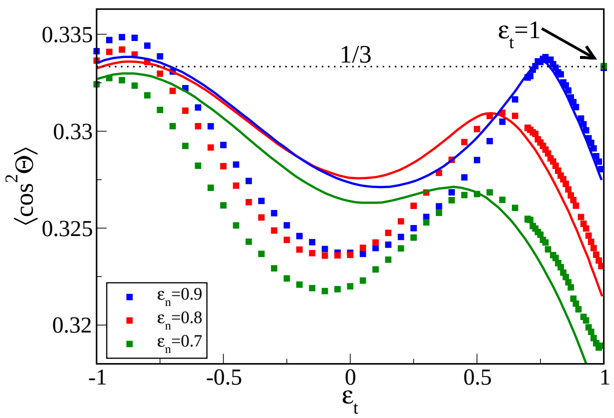

FIG. 2: (Color online) Steady-state value of $\left\langle \cos^2\theta \right\rangle_\infty$ as a function of the coefficient of tangential restitution, ε_t, for different ε_n. The predictions of the analytical theory, Eq. (32), are depicted by lines and points indicate the simulation data by DSMC. The line of vanishing correlations, $\left\langle \cos^2\theta \right\rangle = 1/3$ is shown, as well as the isolated point $\varepsilon_t = 1$, which refers to the system of perfectly smooth hard spheres. Note the existence of non-vanishing correlations even in the limit of smooth spheres, $\varepsilon_t \to 1$ (see Eq. 33).

Decreasing the moment of inertia, q, turns the magnitude of the correlations more sensitive to changes in the coefficients of tangential restitution, as one can see from Fig. 3. Interestingly, varying the moment of inertia can even alter the type of the correlations: For instance, for $q = 1/5$ there exists a region for $\varepsilon_t > 0$, where the rotation axis is preferably directed along the linear velocity, $\left\langle \cos^2\theta \right\rangle_\infty > 1/3$, while for $q = 2/3$ there is no such region.

Fig. 4 (upper panel) illustrates the analytical result, Eq. (32) for the whole range of parameters ε_t and ε_n. Note that for the majority of values of the coefficients, $\left\langle \cos^2\theta \right\rangle_\infty < 1/3$, that is, in most cases the axes tend to be perpendicular to each other. Only in two small regions of the parameter space the axes are preferably parallel. The correlations vanish only for combinations of ε_n and ε_t indicated by full lines. Dashed lines show curves of constant r. Strong correlations appear for large deviations from equipartition. This is shown more clearly in the middle and bottom panels of Fig. 4 which demonstrate the rather strong influence of the moment of inertia I on the correlation factor $\left\langle \cos^2\theta \right\rangle_\infty$.

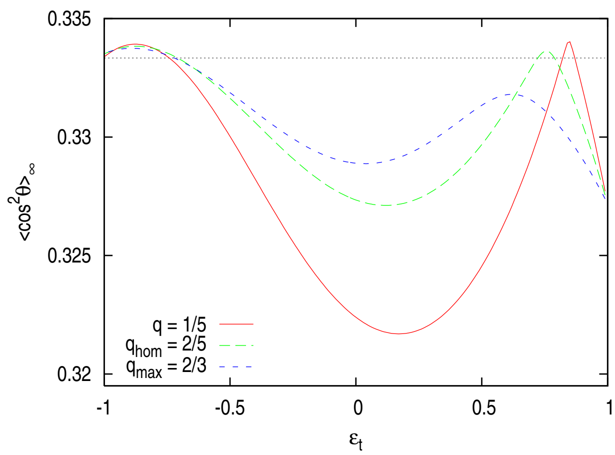

FIG. 3: Steady-state value of $\langle\cos^2\theta\rangle_\infty$ for $\varepsilon_n = 0.9$ as a function of ε_t and for different moments of inertia of a grain (see also Fig. 8). With the decreasing moment of inertia the correlations become more sensitive to variations of the coefficient of tangential restitution

To check the assumption that strong correlations occur for strong deviations from equipartition, we plot in Fig. 5 the correlation factor $\langle\cos^2\theta\rangle_\infty$ as a function of r_∞ and ε_t. Technically this may be done, using $\varepsilon_n = \varepsilon_n(r_\infty)$–the inverse function of $r_\infty = r_\infty(\varepsilon_n)$, given by Eq. (29), for each fixed ε_t. Note that pronounced correlations are present mainly for strong dissipation and large temperature ratios. Also note the small range of admissible temperature ratios for very rough spheres.

Analyzing Eq. (32) in the limit of vanishing roughness,

$$K^{(0)} \equiv \lim_{\varepsilon_t\to 1} \langle\cos^2\theta\rangle_\infty - \frac{1}{3} = -\frac{3}{8}\frac{1-\varepsilon_n}{7-\varepsilon_n} \tag{33}$$

we see that even the smallest roughness induces finite correlations, for any given (fixed) value of the coefficient of normal restitution, $\varepsilon_n \neq 1$. For $\varepsilon_t = 1$, that is, for perfectly smooth spheres, the initial rotational velocity of the particles is preserved. Therefore, the initial rotational energy is preserved as well and r does not reach a steady state. On the other hand $\langle\cos^2\theta\rangle$ relaxes to the stationary value $^1/_3$ once the correlations in the initial values of the translational velocities are lost due to collisions. Hence a straightforward expansion around $\varepsilon_t = 1$ is problematic, or at least should be done with much care, as long as there is a finite inelasticity $\varepsilon_n \neq 1$. [See also the discussion of relaxation times in the following paragraph.]

B. Relaxation to the steady-state

So far we have discussed the quasi-stationary state, which is characterized by constant r and $\langle\cos^2\theta\rangle$. It is also of interest to understand, how this stationary state is reached—starting from arbitrary initial conditions.

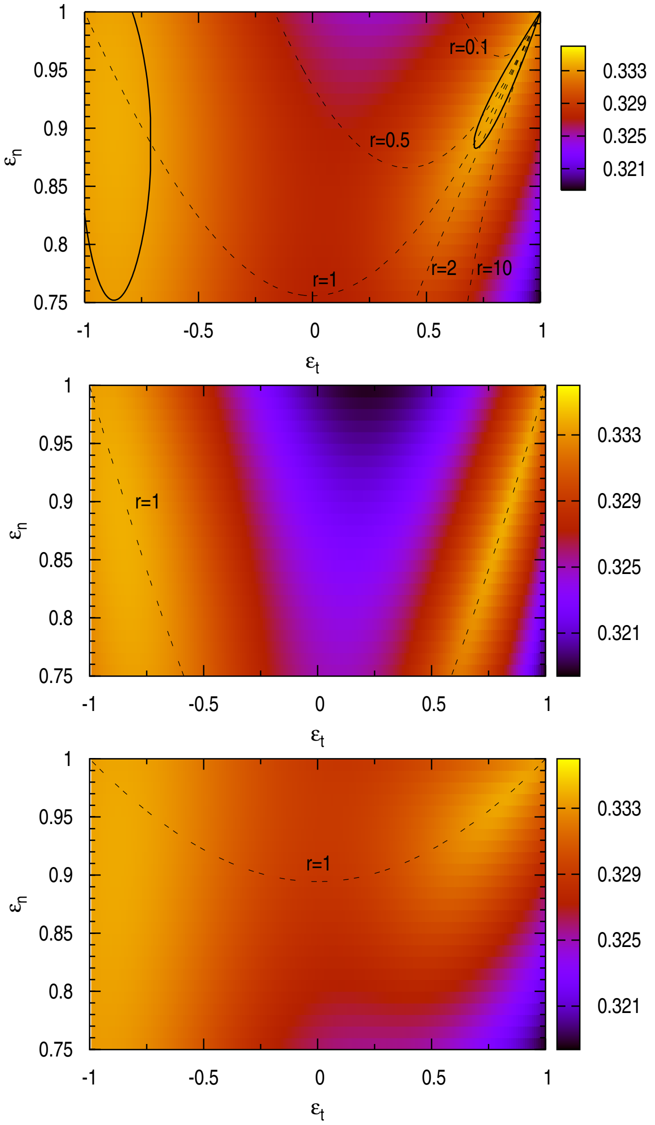

FIG. 4: Stationary value $\langle\cos^2\theta\rangle_\infty$ (color coded) as a function of normal (ε_n) and tangential (ε_t) coefficients of restitution. The stationary value of the temperature ratio r is superimposed through the dashed contour lines. The solid lines indicate vanishing correlations ($\langle\cos\theta\rangle_\infty = 1/3$). The moment of inertia $q = 2/5$ (upper panel) corresponds to homogeneous spheres. The middle and bottom panel show the same data for $q = 1/5$ and $q = 2/3$, respectively

Of particular interest is the limit of almost smooth spheres $\eta_t \propto \varepsilon_t - 1 \ll 1$ [see the definition, Eq. (5)]. While the decay of the rotational temperature R and the translational temperature T takes place extremely slowly, that is, with a rate $\sim \eta_t \ll 1$ [see Eq. (22) with $r = R/T \simeq A/B$ in this limit], the relaxation of the temperature ratio, $r = R/T$ as well as of the correlation factor $x \sim (\langle\cos^2\theta\rangle - 1/3)$ occurs on the collision time scale. Indeed, in this limit one can write using Eqs. (27),

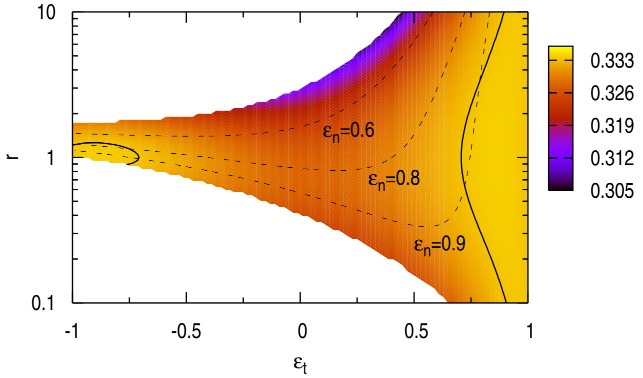

FIG. 5: Stationary value of $\left\langle\cos^2\theta\right\rangle_\infty$ (color coded) as a function of the temperature ratio r_∞ and the coefficient of tangential restitution ε_t. As previously, the solid lines indicate vanishing correlations and the dashed lines follow constant values of the coefficient of normal restitution ε_n. Note the logarithmic scale for the r-axis. The ragged border is an artifact of the limited numerical resolution

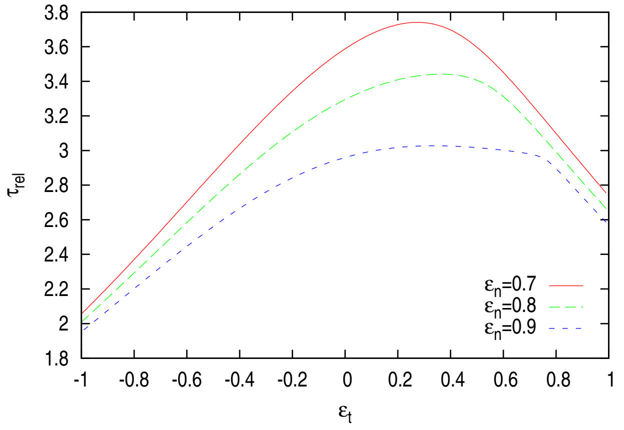

FIG. 6: Relaxation time $\tau_{\rm rel}$ (in the collision units) of $\left\langle\cos^2\theta\right\rangle_\tau$ when it approaches the steady-state value $\left\langle\cos^2\theta\right\rangle_\infty$. Note the narrow range of possible values for $\tau_{\rm rel}$

(28) and the definitions of the coefficients (23) (25),

$$dr/d\tau \simeq -\eta_n(1-\eta_n)\left(r/r_\infty^{(0)}\right)\left(r-r_\infty^{(0)}\right),$$

with $r_\infty^{(0)} \simeq A/B \sim 1/\eta_t^2 \gg 1$ from Eq. (29). This implies that r relaxes to its stationary value exponentially fast with a rate $\eta_n(1-\eta_n) = \mathcal{O}(1)$ (that is, on the collision time scale), while both temperatures T and R continue to decay with the same small rate.

To analyse the relaxation of $x(\tau)$ to its steady state value, we use Eq. (28) and approximate $r(\tau)$ by its steady state value r_∞:

$$\frac{dx}{d\tau} = -a_0 - a_1 x - a_2 x^2 \tag{34}$$

where

$$\begin{aligned} a_0 &= \frac{1}{20}\left[A^{(0)} + B^{(0)} r_\infty + C^{(0)} r_\infty^{-1}\right] \\ a_1 &= \left[\frac{1}{20}A^{(1)} + \frac{1}{20}B^{(1)} r_\infty - A - C + B(r_\infty + r_\infty^{-1})\right] \\ a_2 &= \frac{1}{2}(C - B r_\infty)\,. \end{aligned} \tag{35}$$

The above equation with the initial condition $x(0) = 0$ is solved by

$$x(\tau) - x_\infty = -\frac{x_\infty}{1-\tanh\phi}\left[1 - \tanh\left(\frac{\tau}{\tau_{\rm rel}} + \phi\right)\right], \tag{36}$$

with the relaxation time

$$\tau_{\rm rel} = \frac{1}{2}\sqrt{a_1^2 - 4a_0 a_2} \tag{37}$$

and $\tanh\phi = a_1/\sqrt{a_1^2 - 4a_0a_2}$. Evaluating the coefficients for typical values of ε_t and ε_n, we find that the relaxation of the correlation factor $\left\langle\cos^2\theta\right\rangle_t$ to its steady-state also occurs within a few collisions per particle. This is illustrated in Fig. 6, where we plot the relaxation time $\tau_{\rm rel}$ given by Eq. (37).

We wish to stress here again, that the relaxation on the collisional time scale to the steady state values applies only to the temperature ratio and the mean square cosine of the angle between linear and angular velocity. For nearly smooth particles, $\varepsilon_t \to 1$, the relaxation of the rotational and translational temperatures is, nevertheless, a very slow process, which proceeds with a small rate, tending to zero as $\varepsilon_t \to 1$.

To demonstrate the existence of several time regimes we discuss in the following an instructive example. We initialize the particles with $\boldsymbol{\omega} = 0$ corresponding to $r = 0$. The collision parameters are $\varepsilon_n = \varepsilon_t = 0.8$ so that the asymptotic value of the ratio of temperatures is $r_\infty > 1$. We expect r to monotonically increase as a function of time—and this is indeed observed as shown in Fig. 7. Now, we can check our hypothesis that correlations are small for values of r close to equipartition. If the hypothesis is correct, we should observe *non-monotonic* behavior of $\left\langle\cos^2\theta\right\rangle_t$. For short times the correlations should be large and of tennis ball type, because grazing collisions are the most effective for spinless particles to gain angular momentum. At intermediate times, when $r \sim 1$, the correlations should be very small or vanishing. In the asymptotic state with $r_\infty > 1$, one should again observe finite correlations.

These three time regimes are clearly born out in the time dependent correlations, shown in Fig. 7: (a) In the short time regime ($0 < t < 10^3$) correlations are strong and $0 < r < 1$. (b) At intermediate times ($10^3 < t < 10^5$) equipartition holds approximately $r \approx 1$ and correlations are small or vanishing. (c) The steady state ($t > 10^6$) is characterized by $r \gg 1$ and finite $\left\langle\cos^2\theta\right\rangle_\infty < 1/3$. The agreement between analytical theory and molecular dynamics is good also for the time-dependent quantities.

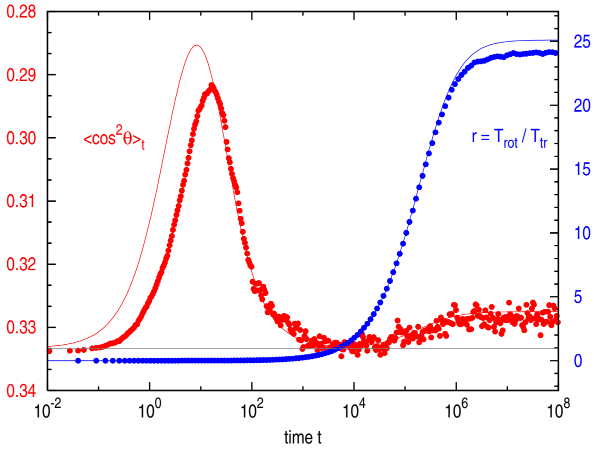

FIG. 7: (Color online) Relaxation of $\left\langle\cos^2\theta\right\rangle_t$ and of the ratio of temperatures $r(t) = R(t)/T(t)$ to the steady state. Dots: molecular dynamics data for 8000 particles, lines: analytical theory. To show that vanishing correlations $\left\langle\cos^2\theta\right\rangle_t$ coincide with equipartition, we have chosen the vertical axes, such that the point $r = 1$ on the right axis (blue) and the point $\left\langle\cos^2\theta\right\rangle_t = 1/3$ on the left axis (red) have the same vertical height as indicated by a horizontal line.

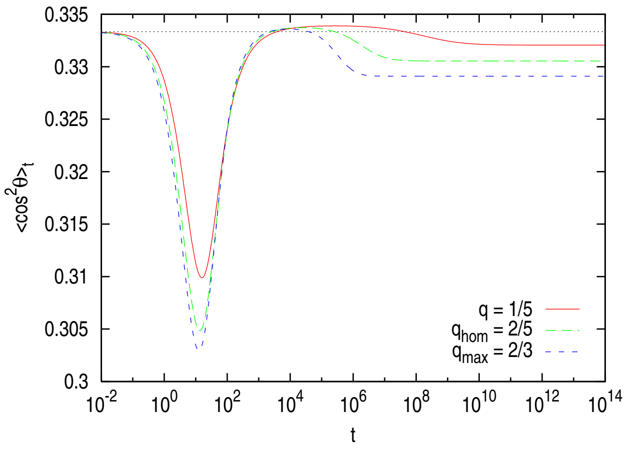

FIG. 8: Impact of the grains' moments of inertia on the evolution and steady-state of $\left\langle\cos^2\theta\right\rangle_t$. The system parameters are $\varepsilon_n = 0.9$, $\varepsilon_t = 0.9$, $r(0) = 0.001$ and vanishing initial correlations. The values of q ($I = qma^2$) represent spheres with the mass concentrated towards the center ($q = 1/5$), the homogeneous spheres ($q = 2/5$) and spheres with the mass concentrated mainly in the outer shell ($q = 2/3$).

Fig. 8 demonstrates that the moment of inertia of the particles does not change the evolution of $\left\langle\cos^2\theta\right\rangle_t$ qualitatively. For the particular choice of the coefficients of restitution the correlations are more pronounced for larger $q = I/ma^2$ and fade with decreasing q. This however is not a general rule; depending on the coefficients ε_n and ε_t, this tendency may reverse.

The correlations between translational and rotational motion also have a noticeable, albeit small impact on the basic characteristics of granular gases—the translational and rotational temperatures. In Fig. 9 we present the time dependence of $R(t)/R^{(0)}(t)$—the ratio of the rotational temperature $R(t)$ with correlations to the corresponding value $R^{(0)}(t)$ without correlations. The respective ratio $T(t)/T^{(0)}(t)$ for the translational temperature is also plotted. Here we choose the case of large $r \simeq 24$ ($\varepsilon_n = \varepsilon_t = 0.8$), which correspond to $\left\langle\cos^2\theta\right\rangle_\infty < 1/3$, that is, for preferably perpendicular rotational and translational velocity. Fig. 9 demonstrates that the effect of the correlations on the granular temperatures $R(t)$ and $T(t)$ is indeed small. The corresponding quantity $r(t) = R(t)/T(t)$ is also not sensitive to these correlations. Moreover $r(t)$ does not deviate noticeably from its steady-state value throughout the system's evolution, that is, $|r(\tau)/r_\infty - 1| \ll 1$, as shown in the inset of Fig. 9.

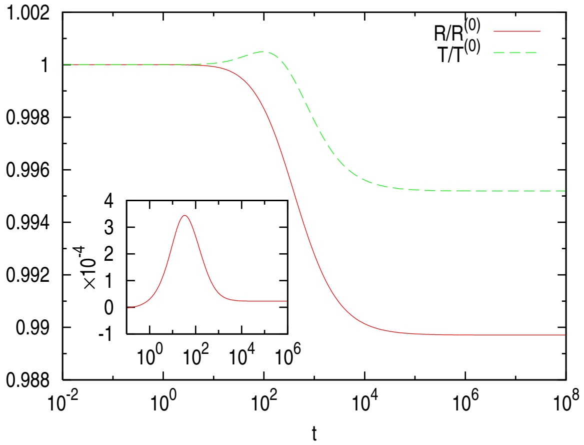

FIG. 9: The ratio of the temperatures calculated with $b(t)$ according to Eq. (24) to those with $b(t) \equiv 0$. The coefficients of restitution are $\varepsilon_n = \varepsilon_t = 0.8$, and the initial ratio of rotational to translational temperatures was set to the steady-state value $r(0) = r_\infty$. The inset shows $r(t)/r(0) - 1$ as a function of time. Note that the deviation of $r(t)$ from r_∞ is always very small.

C. Beyond the second moment

A complete one-particle picture includes the distribution

$$\mathcal{W}(\cos\theta, v, \omega) = \frac{1}{N}\sum_{i=1}^{N}\delta(\cos\theta - \cos\theta_i)\delta(v - v_i)\delta(\omega - \omega_i). \tag{38}$$

Since correlations are developed in collisions, one intuitively expects that particles with larger velocities, that suffer stronger collisions, would show more pronounced orientational correlations; we study these effects by binning the particles velocities.

So far we discussed the correlation factor $\left\langle\cos^2\theta\right\rangle_t$, which is a second moment of the distribution function $\mathcal{W}(\cos\theta, v, \omega)$. Let us now analyze the distribution func-

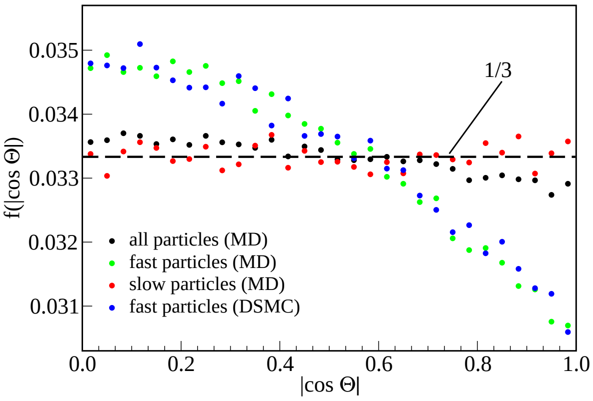

FIG. 10: The angular distribution $f(|\cos\theta|)$ for the system of rough spheres with $\varepsilon_t = 0.9$, $\varepsilon_n = 0.9$ and $q = 2/5$ in the stationary state. Note that while there is no preferable angle between $\boldsymbol{v}$ and $\boldsymbol{\omega}$ for slow particles, correlations are clearly visible for fast particles favouring perpendicular linear and angular velocities.

tion itself. Due to the limited statistics of our numerical data we discriminate only between two classes of particles: the class of fast particles comprising those particles whose linear velocity belongs to the set of the 1/3 largest values *and* whose angular velocity belongs to the set of the 1/3 largest values. The class of slow particles is defined correspondingly as the set of particles whose linear velocity belongs to the set of the 1/3 smallest values *and* the angular velocity belongs to the set of the 1/3 smallest values. In Fig. 10 we show the distributions $f(|\cos\theta|)$ for the two classes in comparison with the distribution for all particles using both methods, MD and DSMC. In both cases we skipped the first 20 collisions per particle such that the ratio of temperatures, r, has reached its stationary value. For the MD simulation we used a system of $N = 10^5$ particles at low density (filling factor $< 1\%$. Then we averaged over 200 snapshots in distance of 1 collision per particle. In case of DSMC we used a system of $N = 10^7$ particles and made the statistics based on a single snapshot. Both results agree very well. The angular distribution is almost flat for slow particles and cannot be distinguished from the distribution of all particles (within statistical accuracy). On the other hand the fast particles exhibit a nonuniform distribution with a maximum around $\cos\theta = 0$. Physically this means that the angle θ between $\boldsymbol{v}$ and $\boldsymbol{\omega}$ for slow particles is uniformly distributed within the interval $(0, \pi)$, while for fast particles it lies preferentially around $\theta = \pi/2$. In other words, for the particular choice of $\varepsilon_t = 0.9$ and $\varepsilon_n = 0.9$ the fast particles tend to behave like sliced tennis balls, with $\boldsymbol{\omega}$ perpendicular to $\boldsymbol{v}$.

VI. CONCLUSIONS AND OUTLOOK

We have analysed in detail the correlations between rotational and translational motion in a granular gas of frictional particles. Under the assumption of molecular chaos and homogeneity we have developed an analytical theory which accounts for the correlations $\left\langle\cos^2\theta\right\rangle_t$ in addition to the rotational $R(t)$ and translational $T(t)$ temperature. We have also performed large scale DSMC simulations as well as event driven simulations to study the evolution of a gas of rough spheres and in particular the above correlations.

We observe that the gas of *rough* particles always relaxes to a steady-state with constant correlation $\left\langle\cos^2\theta\right\rangle_\infty$ and constant ratio $r_\infty = R(t)/T(t)$. While the relaxation of $\left\langle\cos^2\theta\right\rangle$ and r to their steady-state values happens on the collisional time scale, the evolution of the rotational and translational temperature in the near-smooth limit $\varepsilon_t \to 1$ is a slow process with a vanishingly small rate $\sim \eta_t \sim (1 - \varepsilon_t) \ll 1$. Physically, this may be explained as follows. In the near-smooth limit the coupling of the rotational modes to the translational ones becomes very weak. The energy of the rotational motion of the particles is almost conserved in collisions and the exchange of energy between the translational and rotational degrees of freedom becomes very slow. Consequently the rotational temperature as well as the translational temperature have a slowly decaying component, governed by this weak exchange of energies. However both temperatures decay with the *same* slow timescale so that their ratio, r, is stationary - after it has reached its steady state on the fast time scale of a few collisions. Simultaneously, $\left\langle\cos^2\theta\right\rangle_t$ relaxes to its steady state with a similar rate of the order of a few collisions. We conclude that the relaxation of the temperature ratio, r, and the angular correlations is rapid, – independent of the strength of the coupling $(1 - \varepsilon_t)$ as long as it is finite. Furthermore the correlations persist up to a vanishingly small roughness and are absent only for perfectly smooth particles, $\varepsilon_t = 1$, which makes expansions around the smooth limit questionable.

Our main results concern the correlation between the directions of rotational and translational velocity in the stationary state: The correlations depend sensitively on the values of the coefficients of restitution and the moment of inertia; for most of the system parameters $\left\langle\cos^2\theta\right\rangle < 1/3$, implying that linear and angular velocities are preferably orthogonal, like in a sliced tennis ball. Only for a small part of the parameter space $\left\langle\cos^2\theta\right\rangle > 1/3$, which means that $\boldsymbol{v}$ and $\boldsymbol{\omega}$ are preferably parallel like in a rifled bullet; the manifold of vanishing correlations (in $\varepsilon_n, \varepsilon_t$ space) has seemingly zero measure. The correlations are more pronounced for strong deviations from equipartition.

Our approach can be extended in several directions. In the simulations it is straightforward to use more advanced models for the coefficients of restitution as functions of the impact velocity, e.g. [38, 39, 40, 41]. It would also be of interest to study the full one-particle distribution. Our results already indicate that more energetic particles have stronger correlations, but a systematic study has yet to be done. Furthermore, one expects to observe correlations not only in very dilute gases, but also in rapidly moving denser systems. Our approximate analytical theory is based on the assumption of homogeneity and the density only enters into the Enskog collision frequency, which sets the time scale. Hence our results for the stationary state are independent of the density. This cannot hold true in a rapidly moving dense system, yet we expect to observe correlations as well. These could be analysed in a molecular dynamics simulation either for a driven [47] or undriven system. Finally, the observed correlations may have important consequences for the stability theory of dilute granular flows: they possibly alter the domain of stability of granular system with respect to shear fluctuations—the main instability of granular flows of smooth particles.

Acknowledgement We thank Isaac Goldhirsch for interesting discussions; TK and AZ thank Timo Aspelmeier for help with the MD simulations; TP acknowledges support by a grant from G.I.F., the German-Israeli Foundation for Scientific Research and Development.

APPENDIX: ANALYTICAL CALCULATIONS

1. Correlation factor

We present the details of the analytical calculations, leading to the three self-consistent equations (22) and (24) for $T(t), R(t)$ and $b(t)$. First, we note that he computation of $b(t)$ or $\left\langle\cos^2\theta\right\rangle_t$ is severely hampered by the denominator in Eq. (9). Fortunately one can carry out the calculations with the auxiliary observable

$$\left\langle\Delta\right\rangle_t \equiv \frac{2}{3N}\sum_{i=1}^{N} \boldsymbol{v}_i^2\boldsymbol{\omega}_i^2 P_2(\cos\theta_i)\,. \tag{A.1}$$

Its relation to our set of observables can be established by essentially the same steps as leading from Eq. (19) to Eq. (21):

$$30b(t)\frac{T(t)R(t)}{qm^2a^2} = \left\langle\Delta\right\rangle_t \frac{qm^2a^2}{T(t)R(t)}\,. \tag{A.2}$$

In the case of vanishing correlations we have $\left\langle\Delta\right\rangle_t = 0$. Positive (negative) values correspond to a preference of a parallel (perpendicular) orientation.

Owing to the assumptions of spatial homogeneity and molecular chaos it suffices to consider the phase space of only a single pair of particles (without loss of generality these shall be labeled 1 and 2). Integrating out the spatial degrees of freedom and using the definition of the pair correlation function

$$N(N-1)\int d\boldsymbol{r}_3\ldots d\boldsymbol{r}_N g_N(\boldsymbol{r}_1,\ldots\boldsymbol{r}_N) = n^2 g_2(r_{12})\,, \tag{A.3}$$

with n being the number density of the gas (e.g. [6]) we obtain

$$\begin{aligned}\left\langle i\mathcal{L}_+ v\Delta\right\rangle_t =& \nu\, N\int\limits_{v_1}\int\limits_{v_2}\int\limits_{\omega_1}\int\limits_{\omega_2}\left(\hat{\boldsymbol{n}}\cdot\boldsymbol{v}_{12}\right)\Theta\left(-\hat{\boldsymbol{n}}\cdot\boldsymbol{v}_{12}\right)\\ &\times\left[1+b(t)\boldsymbol{v}_1^2\boldsymbol{\omega}_1^2P_2\left(\cos\theta_1\right)\right]\\ &\times\left[1+b(t)\boldsymbol{v}_2^2\boldsymbol{\omega}_2^2P_2\left(\cos\theta_2\right)\right]\\ &\times\left(\hat{b}_{12}-1\right)\Delta\,,\end{aligned} \tag{A.4}$$

where $\hat{\boldsymbol{n}}$ is an arbitrary but fixed unit vector, $\nu = -8\pi na^2g_2(2a)$ and we used the shorthand notations

$$\begin{aligned}\int\limits_{v_i} &\equiv \left(\frac{m}{2\pi T}\right)^{3/2}\int d^3v_i\exp\left(-\frac{m\boldsymbol{v}_i^2}{2T}\right)\\ \int\limits_{\omega_i} &\equiv \left(\frac{I}{2\pi R}\right)^{3/2}\int d^3\omega_i\exp\left(-\frac{I\boldsymbol{\omega}_i^2}{2R}\right)\,.\end{aligned} \tag{A.5}$$

In the following we will drop the $b^2(t)$-term stemming from the product of the two one particle distribution functions ρ_1 since it was assumed to be small and we only want to go to first order in $b(t)$.

The calculation of $\left(\hat{b}_{12}-1\right)\Delta$ is obviously rather involved and, thus, it needs to be broken up to stay tractable. It is convenient to introduce relative integration variables

$$\begin{aligned}\boldsymbol{v} &\equiv \boldsymbol{v}_{12}/\sqrt{2} \qquad \boldsymbol{V} \equiv (\boldsymbol{v}_1+\boldsymbol{v}_2)/\sqrt{2}\\ \boldsymbol{\omega} &\equiv \boldsymbol{\omega}_{12}/\sqrt{2} \qquad \boldsymbol{\Omega} \equiv (\boldsymbol{\omega}_1+\boldsymbol{\omega}_2)/\sqrt{2}\,.\end{aligned} \tag{A.6}$$

The term $\left\langle i\mathcal{L}_+\Delta\right\rangle_t$ can be broken up along two different principles. First, one can make the dependence on $b(t)$ explicit, that is,

$$\begin{aligned}\left\langle i\mathcal{L}_+\Delta\right\rangle_t =& \left\langle\left(\hat{b}_{12}-1\right)\Delta\right\rangle^{(0)}\\ &+ b(t)\left\langle\left(\hat{b}_{12}-1\right)\Delta\right\rangle^{(1)} + \mathcal{O}\left(b^2\right)\,,\end{aligned} \tag{A.7}$$

where for any function F

$$\left\langle F\right\rangle^{(0)} = \nu\int\limits_{v_1}\int\limits_{v_2}\int\limits_{\omega_1}\int\limits_{\omega_2}\left(\hat{\boldsymbol{n}}\cdot\boldsymbol{v}_{12}\right)\Theta\left(-\hat{\boldsymbol{n}}\cdot\boldsymbol{v}_{12}\right)\,F \tag{A.8}$$

and

$$\begin{aligned}\left\langle F\right\rangle^{(1)} =& \nu\int\limits_{v_1}\int\limits_{v_2}\int\limits_{\omega_1}\int\limits_{\omega_2}\left(\hat{\boldsymbol{n}}\cdot\boldsymbol{v}_{12}\right)\Theta\left(-\hat{\boldsymbol{n}}\cdot\boldsymbol{v}_{12}\right)\\ &\times\left[\boldsymbol{v}_1^2\boldsymbol{\omega}_1^2P_2\left(\cos\theta_1\right)+\boldsymbol{v}_2^2\boldsymbol{\omega}_2^2P_2\left(\cos\theta_2\right)\right]\,F\,.\end{aligned} \tag{A.9}$$

In order to be able to exploit some further symmetries it is advisable to split up the last average again,

$$\left\langle F\right\rangle^{(1)} = \left\langle F\right\rangle^{\text{even}} + \left\langle F\right\rangle^{\text{odd}} \tag{A.10}$$

where

$$\begin{aligned}\langle F\rangle^{\text{even}} = \frac{3\sqrt{2}}{4}\nu \int\limits_{v}\int\limits_{V}\int\limits_{\omega}\int\limits_{\Omega} (\hat{\boldsymbol{n}}\cdot\boldsymbol{v})\,\Theta\left(-\hat{\boldsymbol{n}}\cdot\boldsymbol{v}\right) \\ \times\Big[(\boldsymbol{V}\cdot\boldsymbol{\Omega})^2+(\boldsymbol{V}\cdot\boldsymbol{\omega})^2 \\ +(\boldsymbol{v}\cdot\boldsymbol{\Omega})^2+(\boldsymbol{v}\cdot\boldsymbol{\omega})^2 \\ -\frac{1}{3}\left(\boldsymbol{V}^2+\boldsymbol{v}^2\right)\left(\boldsymbol{\Omega}^2+\boldsymbol{\omega}^2\right)\Big]\,F \quad \text{(A.11)}\end{aligned}$$

involves only even powers of $\boldsymbol{V},\boldsymbol{\omega},\boldsymbol{\Omega}$ and

$$\begin{aligned}\langle F\rangle^{\text{odd}} = \frac{3\sqrt{2}}{2}\nu \int\limits_{v}\int\limits_{V}\int\limits_{\omega}\int\limits_{\Omega} (\hat{\boldsymbol{n}}\cdot\boldsymbol{v})\,\Theta\left(-\hat{\boldsymbol{n}}\cdot\boldsymbol{v}\right) \\ \times\Big[(\boldsymbol{V}\cdot\boldsymbol{\Omega})(\boldsymbol{v}\cdot\boldsymbol{\omega})+(\boldsymbol{V}\cdot\boldsymbol{\omega})(\boldsymbol{v}\cdot\boldsymbol{\Omega}) \\ -\frac{2}{3}(\boldsymbol{V}\cdot\boldsymbol{v})(\boldsymbol{\Omega}\cdot\boldsymbol{\omega})\Big]\,F \quad \text{(A.12)}\end{aligned}$$

in contrast involves only the odd powers of these quantities.

Independently we can write

$$\Delta = \Delta_A - \Delta_B/3 \tag{A.13}$$

where

$$\Delta_A \equiv \sum_i (\boldsymbol{v}_i\cdot\boldsymbol{\omega}_i)^2 \quad \text{and} \quad \Delta_B \equiv \sum_i \boldsymbol{v}_i^2\boldsymbol{\omega}_i^2\,. \tag{A.14}$$

First we address the Δ_A-part. Applying the collision rule to Δ_A yields

$$\begin{aligned}\left(\hat{b}_{12}-1\right)\Delta_A &= (\boldsymbol{\delta}\cdot\boldsymbol{\omega})^2+(\boldsymbol{\delta}\cdot\boldsymbol{\Omega})^2+\frac{1}{q^2a^2}\left[(\hat{\boldsymbol{n}}\times\boldsymbol{\delta})\cdot\boldsymbol{v}\right]^2+\frac{1}{q^2a^2}\left[(\hat{\boldsymbol{n}}\times\boldsymbol{\delta})\cdot\boldsymbol{V}\right]^2-\sqrt{2}\,(\boldsymbol{\delta}\cdot\boldsymbol{\Omega})(\boldsymbol{v}\cdot\boldsymbol{\Omega}) \\ &\quad-\sqrt{2}\,(\boldsymbol{\delta}\cdot\boldsymbol{\Omega})(\boldsymbol{V}\cdot\boldsymbol{\omega})-\sqrt{2}\,(\boldsymbol{\delta}\cdot\boldsymbol{\omega})(\boldsymbol{v}\cdot\boldsymbol{\omega})-\sqrt{2}\,(\boldsymbol{\delta}\cdot\boldsymbol{\omega})(\boldsymbol{V}\cdot\boldsymbol{\Omega})+\frac{\sqrt{2}}{qa}(\boldsymbol{v}\cdot\boldsymbol{\Omega})(\hat{\boldsymbol{n}}\times\boldsymbol{\delta})\cdot\boldsymbol{v} \\ &\quad+\frac{\sqrt{2}}{qa}(\boldsymbol{V}\cdot\boldsymbol{\omega})(\hat{\boldsymbol{n}}\times\boldsymbol{\delta})\cdot\boldsymbol{v}+\frac{\sqrt{2}}{qa}(\boldsymbol{v}\cdot\boldsymbol{\omega})(\hat{\boldsymbol{n}}\times\boldsymbol{\delta})\cdot\boldsymbol{V}+\frac{\sqrt{2}}{qa}(\boldsymbol{V}\cdot\boldsymbol{\Omega})(\hat{\boldsymbol{n}}\times\boldsymbol{\delta})\cdot\boldsymbol{V} \\ &\quad-\frac{2}{qa}(\boldsymbol{\delta}\cdot\boldsymbol{\Omega})(\hat{\boldsymbol{n}}\times\boldsymbol{\delta})\cdot\boldsymbol{v}-\frac{2}{qa}(\boldsymbol{\delta}\cdot\boldsymbol{\omega})(\hat{\boldsymbol{n}}\times\boldsymbol{\delta})\cdot\boldsymbol{V}\end{aligned} \tag{A.15}$$

and invoking the definition of $\boldsymbol{\delta}$, Eq. (4), we obtain

$$\begin{aligned}\left\langle\left(\hat{b}_{12}-1\right)\Delta_A\right\rangle^{(0)} &= 2\left(2\eta_t^2-2\eta_t+\frac{\eta_t^2}{q^2}-\frac{\eta_t}{q}+\frac{2\eta_t^2}{q}\right)\left\langle(\boldsymbol{v}\cdot\boldsymbol{\omega})^2\right\rangle^{(0)}+2\frac{\eta_t}{q}\left(\frac{\eta_t}{q}-1\right)\left\langle(\boldsymbol{\omega}\cdot\boldsymbol{V})^2\right\rangle^{(0)} \\ &\quad+2\left[2(\eta_n-\eta_t)^2+\frac{\eta_t^2}{q^2}-\frac{2\eta_t}{q}(\eta_n-\eta_t)\right]\left\langle(\hat{\boldsymbol{n}}\cdot\boldsymbol{v})^2(\hat{\boldsymbol{n}}\cdot\boldsymbol{\omega})^2\right\rangle^{(0)} \\ &\quad+2\frac{\eta_t^2}{q^2}\left\langle(\hat{\boldsymbol{n}}\cdot\boldsymbol{V})^2(\hat{\boldsymbol{n}}\cdot\boldsymbol{\omega})^2\right\rangle^{(0)}+2\eta_t^2a^2\left\langle\left[(\hat{\boldsymbol{n}}\times\boldsymbol{\Omega})\cdot\boldsymbol{\omega}\right]^2\right\rangle^{(0)}+2\frac{\eta_t^2}{q^2a^2}\left\langle\left[(\hat{\boldsymbol{n}}\times\boldsymbol{v})\cdot\boldsymbol{V}\right]^2\right\rangle^{(0)} \\ &\quad+4\left[(2\eta_t-1)(\eta_n-\eta_t)-\frac{\eta_t^2}{q^2}+\frac{1}{2}\frac{\eta_t}{q}-\frac{\eta_t^2}{q}+\frac{\eta_t}{q}(\eta_n-\eta_t)\right]\left\langle(\hat{\boldsymbol{n}}\cdot\boldsymbol{v})(\hat{\boldsymbol{n}}\cdot\boldsymbol{\omega})(\boldsymbol{v}\cdot\boldsymbol{\omega})\right\rangle^{(0)} \\ &\quad-\frac{2\eta_t}{q}\left(\frac{2\eta_t}{q}-1\right)\left\langle(\hat{\boldsymbol{n}}\cdot\boldsymbol{V})(\hat{\boldsymbol{n}}\cdot\boldsymbol{\omega})(\boldsymbol{V}\cdot\boldsymbol{\omega})\right\rangle^{(0)}\,.\end{aligned} \tag{A.16}$$

The terms that vanish by symmetry are already left out at this point. The contributions to $\left\langle\left(\hat{b}_{12}-1\right)\Delta_A\right\rangle^{\text{even}}$ have exactly the same form.

For $\left\langle \left(\hat{b}_{12}-1\right)\Delta_A\right\rangle^{\mathrm{odd}}$ one finds the following contributions

$$\begin{aligned}\left\langle \left(\hat{b}_{12}-1\right)\Delta_A\right\rangle^{\mathrm{odd}} &= \left(\frac{4\eta_t^2}{q}-\frac{4\eta_t}{q}-4\eta_t\right)\left\langle (\boldsymbol{v}\cdot\boldsymbol{\omega})(\boldsymbol{V}\cdot\boldsymbol{\Omega})\right\rangle^{\mathrm{odd}} - \frac{4\eta_t}{q}(\eta_n-\eta_t)\left\langle (\hat{\boldsymbol{n}}\cdot\boldsymbol{v})(\hat{\boldsymbol{n}}\cdot\boldsymbol{V})(\hat{\boldsymbol{n}}\cdot\boldsymbol{\omega})(\hat{\boldsymbol{n}}\cdot\boldsymbol{\Omega})\right\rangle^{\mathrm{odd}} \\ &\quad + \frac{2\eta_t}{q}(1-2\eta_t)\left\langle (\hat{\boldsymbol{n}}\cdot\boldsymbol{V})(\hat{\boldsymbol{n}}\cdot\boldsymbol{\Omega})(\boldsymbol{v}\cdot\boldsymbol{\omega})\right\rangle^{\mathrm{odd}} - \frac{4\eta_t^2}{q}\left\langle [(\hat{\boldsymbol{n}}\times\boldsymbol{v})\cdot\boldsymbol{V}]\,[(\hat{\boldsymbol{n}}\times\boldsymbol{\Omega})\cdot\boldsymbol{\omega}]\right\rangle^{\mathrm{odd}} \\ &\quad + \left[4\left(\frac{\eta_t}{q}-1\right)(\eta_n-\eta_t)+\frac{2\eta_t}{q}\right]\left\langle (\hat{\boldsymbol{n}}\cdot\boldsymbol{v})(\hat{\boldsymbol{n}}\cdot\boldsymbol{\omega})(\boldsymbol{V}\cdot\boldsymbol{\Omega})\right\rangle^{\mathrm{odd}}\,. \qquad \text{(A.17)}\end{aligned}$$

Correspondingly, the Δ_B-part may be written as

$$\begin{aligned}\left\langle \left(\hat{b}_{12}-1\right)\Delta_B\right\rangle^{(0)} &= \frac{2\eta_t}{q}\left(\frac{\eta_t}{q}-1\right)(2\eta_t-1)^2\left\langle \boldsymbol{v}^2(\boldsymbol{n}\times\boldsymbol{\Omega})^2\right\rangle^{(0)} + \frac{2\eta_t}{q}\left(\frac{\eta_t}{q}-1\right)\left\langle \boldsymbol{V}^2(\boldsymbol{n}\times\boldsymbol{\Omega})^2\right\rangle^{(0)} \\ &\quad + \frac{2\eta_t^2}{q^2a^2}(2\eta_t-1)^2\left\langle \boldsymbol{v}^2(\hat{\boldsymbol{n}}\times\boldsymbol{v})^2\right\rangle^{(0)} + \frac{2\eta_t^2}{q^2a^2}\left\langle \boldsymbol{V}^2(\hat{\boldsymbol{n}}\times\boldsymbol{v})^2\right\rangle^{(0)} + 4\eta_t(\eta_t-1)\left\langle \boldsymbol{v}^2\boldsymbol{\omega}^2\right\rangle^{(0)} \\ &\quad + 4\left(\eta_n^2-\eta_n-\eta_t^2+\eta_t\right)\left\langle (\hat{\boldsymbol{n}}\cdot\boldsymbol{v})^2\boldsymbol{\omega}^2\right\rangle^{(0)} + \frac{8\eta_t}{q}\left(\frac{\eta_t}{q}-1\right)\left(\eta_n^2-\eta_n-\eta_t^2+\eta_t\right)\left\langle (\hat{\boldsymbol{n}}\cdot\boldsymbol{v})^2(\hat{\boldsymbol{n}}\times\boldsymbol{\Omega})^2\right\rangle^{(0)} \\ &\quad + \frac{8\eta_t^2}{q}\left(\frac{2\eta_t}{q}-1\right)(2\eta_t-1)\left\langle [(\hat{\boldsymbol{n}}\times\boldsymbol{v})\cdot\boldsymbol{\Omega}]^2\right\rangle^{(0)} + \frac{8\eta_t^2}{q^2a^2}\left(\eta_n^2-\eta_n-\eta_t^2+\eta_t\right)\left\langle (\hat{\boldsymbol{n}}\cdot\boldsymbol{v})^2(\hat{\boldsymbol{n}}\times\boldsymbol{v})^2\right\rangle^{(0)} \\ &\quad + 2\eta_t^2a^2\left\langle (\hat{\boldsymbol{n}}\times\boldsymbol{\Omega})^2\boldsymbol{\omega}^2\right\rangle^{(0)} + 2\eta_t^2a^2\left\langle (\hat{\boldsymbol{n}}\times\boldsymbol{\Omega})^2\boldsymbol{\Omega}^2\right\rangle^{(0)} + \frac{8\eta_t^3}{q}a^2\left(\frac{\eta_t}{q}-1\right)\left\langle (\hat{\boldsymbol{n}}\times\boldsymbol{\Omega})^4\right\rangle^{(0)} \\ &\quad + \frac{8\eta_t^4}{q^2}\left\langle (\hat{\boldsymbol{n}}\times\boldsymbol{\Omega})^2(\hat{\boldsymbol{n}}\times\boldsymbol{v})^2\right\rangle^{(0)}\,. \qquad \text{(A.18)}\end{aligned}$$

The contributions to $\left\langle \left(\hat{b}_{12}-1\right)\Delta_B\right\rangle^{\mathrm{even}}$ again are formally equivalent to the above expression. This leaves us with

$$\begin{aligned}\left\langle \left(\hat{b}_{12}-1\right)\Delta_B\right\rangle^{\mathrm{odd}} &= -\frac{4\eta_t}{q}(2\eta_t-1)\left\langle (\hat{\boldsymbol{n}}\cdot\boldsymbol{\omega})(\hat{\boldsymbol{n}}\cdot\boldsymbol{\Omega})(\boldsymbol{v}\cdot\boldsymbol{V})\right\rangle^{\mathrm{odd}} + \frac{8\eta_t^2}{q}\left\langle [(\hat{\boldsymbol{n}}\times\boldsymbol{v})\cdot\boldsymbol{\omega}]\,[(\hat{\boldsymbol{n}}\times\boldsymbol{\Omega})\cdot\boldsymbol{V}]\right\rangle^{\mathrm{odd}} \\ &\quad - \frac{8\eta_t}{q}(\eta_n-\eta_t)\left\langle (\hat{\boldsymbol{n}}\cdot\boldsymbol{v})(\hat{\boldsymbol{n}}\cdot\boldsymbol{V})(\hat{\boldsymbol{n}}\cdot\boldsymbol{\omega})(\hat{\boldsymbol{n}}\cdot\boldsymbol{\Omega})\right\rangle^{\mathrm{odd}}\,. \qquad \text{(A.19)}\end{aligned}$$

We have now reduced the problem to the tedious but straightforward calculation of a considerable number of averages. This task is best suited for a computer algebra system and thus we only tabulate the results. To simplify the notation we introduce the abbreviations $\tilde{\nu}\equiv\nu\sqrt{T/m\pi}$, $\tilde{T}\equiv T/m$, and $\tilde{R}\equiv R/I$

$$\left\langle (\boldsymbol{v}\cdot\boldsymbol{\omega})^2\right\rangle^{(0)} = -4\tilde{\nu}\tilde{T}\tilde{R} \qquad \text{(A.20a)}$$

$$\left\langle (\boldsymbol{V}\cdot\boldsymbol{\omega})^2\right\rangle^{(0)} = -3\tilde{\nu}\tilde{T}\tilde{R} \qquad \text{(A.20b)}$$

$$\left\langle (\hat{\boldsymbol{n}}\cdot\boldsymbol{v})^2(\hat{\boldsymbol{n}}\cdot\boldsymbol{\omega})^2\right\rangle^{(0)} = -2\tilde{\nu}\tilde{T}\tilde{R} \qquad \text{(A.20c)}$$

$$\left\langle (\hat{\boldsymbol{n}}\cdot\boldsymbol{V})^2(\hat{\boldsymbol{n}}\cdot\boldsymbol{\omega})^2\right\rangle^{(0)} = -\tilde{\nu}\tilde{T}\tilde{R} \qquad \text{(A.20d)}$$

$$\left\langle [(\hat{\boldsymbol{n}}\times\boldsymbol{\Omega})\cdot\boldsymbol{\omega}]^2\right\rangle^{(0)} = -2\tilde{\nu}\tilde{R}^2 \qquad \text{(A.20e)}$$

$$\left\langle [(\hat{\boldsymbol{n}}\times\boldsymbol{v})\cdot\boldsymbol{V}]^2\right\rangle^{(0)} = -2\tilde{\nu}\tilde{T}^2 \qquad \text{(A.20f)}$$

$$\left\langle (\hat{\boldsymbol{n}}\cdot\boldsymbol{v})(\hat{\boldsymbol{n}}\cdot\boldsymbol{\omega})(\boldsymbol{v}\cdot\boldsymbol{\omega})\right\rangle^{(0)} = -2\tilde{\nu}\tilde{T}\tilde{R} \qquad \text{(A.20g)}$$

$$\left\langle (\hat{\boldsymbol{n}}\cdot\boldsymbol{V})(\hat{\boldsymbol{n}}\cdot\boldsymbol{\omega})(\boldsymbol{V}\cdot\boldsymbol{\omega})\right\rangle^{(0)} = -\tilde{\nu}\tilde{T}\tilde{R} \qquad \text{(A.20h)}$$

$$\left\langle \boldsymbol{v}^2(\hat{\boldsymbol{n}}\times\boldsymbol{\Omega})^2\right\rangle^{(0)} = -8\tilde{\nu}\tilde{T}\tilde{R} \qquad \text{(A.20i)}$$

$$\left\langle \boldsymbol{V}^2(\hat{\boldsymbol{n}}\times\boldsymbol{\Omega})^2\right\rangle^{(0)} = -6\tilde{\nu}\tilde{T}\tilde{R} \qquad \text{(A.20j)}$$

$$\left\langle \boldsymbol{v}^2(\hat{\boldsymbol{n}}\times\boldsymbol{v})^2\right\rangle^{(0)} = -12\tilde{\nu}\tilde{T}^2 \qquad \text{(A.20k)}$$

$$\left\langle \boldsymbol{V}^2(\hat{\boldsymbol{n}}\times\boldsymbol{v})^2\right\rangle^{(0)} = -6\tilde{\nu}\tilde{T}^2 \qquad \text{(A.20l)}$$

$$\left\langle \boldsymbol{v}^2 \boldsymbol{\omega}^2 \right\rangle^{(0)} = -12\tilde{\nu}\tilde{T}\tilde{R} \tag{A.20m}$$

$$\left\langle (\hat{\boldsymbol{n}} \cdot \boldsymbol{v})^2 \boldsymbol{\omega}^2 \right\rangle^{(0)} = -6\tilde{\nu}\tilde{T}\tilde{R} \tag{A.20n}$$

$$\left\langle (\hat{\boldsymbol{n}} \cdot \boldsymbol{v})^2 (\hat{\boldsymbol{n}} \times \boldsymbol{\Omega})^2 \right\rangle^{(0)} = -4\tilde{\nu}\tilde{T}\tilde{R} \tag{A.20o}$$

$$\left\langle [(\hat{\boldsymbol{n}} \times \boldsymbol{v}) \cdot \boldsymbol{\Omega}]^2 \right\rangle^{(0)} = -2\tilde{\nu}\tilde{T}\tilde{R} \tag{A.20p}$$

$$\left\langle (\hat{\boldsymbol{n}} \cdot \boldsymbol{v})^2 (\hat{\boldsymbol{n}} \times \boldsymbol{v})^2 \right\rangle^{(0)} = -4\tilde{\nu}\tilde{T}^2 \tag{A.20q}$$

$$\left\langle (\hat{\boldsymbol{n}} \times \boldsymbol{\Omega})^2 \boldsymbol{\omega}^2 \right\rangle^{(0)} = -6\tilde{\nu}\tilde{R}^2 \tag{A.20r}$$

$$\left\langle (\hat{\boldsymbol{n}} \times \boldsymbol{\Omega})^2 \boldsymbol{\Omega}^2 \right\rangle^{(0)} = -10\tilde{\nu}\tilde{R}^2 \tag{A.20s}$$

$$\left\langle (\hat{\boldsymbol{n}} \times \boldsymbol{\Omega})^4 \right\rangle^{(0)} = -8\tilde{\nu}\tilde{R}^2 \tag{A.20t}$$

$$\left\langle (\hat{\boldsymbol{n}} \times \boldsymbol{\Omega})^2 (\hat{\boldsymbol{n}} \times \boldsymbol{v})^2 \right\rangle^{(0)} = -4\tilde{\nu}\tilde{T}\tilde{R} \tag{A.20u}$$

$$\left\langle (\boldsymbol{v} \cdot \boldsymbol{\omega})^2 \right\rangle^{\mathrm{even}} = -24\tilde{\nu}\tilde{T}^2\tilde{R}^2 \tag{A.21a}$$

$$\left\langle (\boldsymbol{V} \cdot \boldsymbol{\omega})^2 \right\rangle^{\mathrm{even}} = -15\tilde{\nu}\tilde{T}^2\tilde{R}^2 \tag{A.21b}$$

$$\left\langle (\hat{\boldsymbol{n}} \cdot \boldsymbol{v})^2 (\hat{\boldsymbol{n}} \cdot \boldsymbol{\omega})^2 \right\rangle^{\mathrm{even}} = -6\tilde{\nu}\tilde{T}^2\tilde{R}^2 \tag{A.21c}$$

$$\left\langle (\hat{\boldsymbol{n}} \cdot \boldsymbol{V})^2 (\hat{\boldsymbol{n}} \cdot \boldsymbol{\omega})^2 \right\rangle^{\mathrm{even}} = -3\tilde{\nu}\tilde{T}^2\tilde{R}^2 \tag{A.21d}$$

$$\left\langle [(\hat{\boldsymbol{n}} \times \boldsymbol{\Omega}) \cdot \boldsymbol{\omega}]^2 \right\rangle^{\mathrm{even}} = 2\tilde{\nu}\tilde{T}\tilde{R}^3 \tag{A.21e}$$

$$\left\langle (\hat{\boldsymbol{n}} \cdot \boldsymbol{v}) (\hat{\boldsymbol{n}} \cdot \boldsymbol{\omega}) (\boldsymbol{v} \cdot \boldsymbol{\omega}) \right\rangle^{\mathrm{even}} = -12\tilde{\nu}\tilde{T}^2\tilde{R}^2 \tag{A.21f}$$

$$\left\langle (\hat{\boldsymbol{n}} \cdot \boldsymbol{V}) (\hat{\boldsymbol{n}} \cdot \boldsymbol{\omega}) (\boldsymbol{V} \cdot \boldsymbol{\omega}) \right\rangle^{\mathrm{even}} = -6\tilde{\nu}\tilde{T}^2\tilde{R}^2 \tag{A.21g}$$

$$\left\langle \boldsymbol{v}^2 (\hat{\boldsymbol{n}} \times \boldsymbol{\Omega})^2 \right\rangle^{\mathrm{even}} = 6\tilde{\nu}\tilde{T}^2\tilde{R}^2 \tag{A.21h}$$

$$\left\langle \boldsymbol{V}^2 (\hat{\boldsymbol{n}} \times \boldsymbol{\Omega})^2 \right\rangle^{\mathrm{even}} = 3\tilde{\nu}\tilde{T}^2\tilde{R}^2 \tag{A.21i}$$

$$\left\langle (\hat{\boldsymbol{n}} \cdot \boldsymbol{v})^2 (\hat{\boldsymbol{n}} \times \boldsymbol{\Omega})^2 \right\rangle^{\mathrm{even}} = 6\tilde{\nu}\tilde{T}^2\tilde{R}^2 \tag{A.21j}$$

$$\left\langle [(\hat{\boldsymbol{n}} \times \boldsymbol{v}) \cdot \boldsymbol{\Omega}]^2 \right\rangle^{\mathrm{even}} = 6\tilde{\nu}\tilde{T}^2\tilde{R}^2 \tag{A.21k}$$

$$\left\langle \boldsymbol{\omega}^2 (\hat{\boldsymbol{n}} \times \boldsymbol{\Omega})^2 \right\rangle^{\mathrm{even}} = 3\tilde{\nu}\tilde{T}\tilde{R}^3 \tag{A.21l}$$

$$\left\langle \boldsymbol{\Omega}^2 (\hat{\boldsymbol{n}} \times \boldsymbol{\Omega})^2 \right\rangle^{\mathrm{even}} = 7\tilde{\nu}\tilde{T}\tilde{R}^3 \tag{A.21m}$$

$$\left\langle (\hat{\boldsymbol{n}} \times \boldsymbol{\Omega})^4 \right\rangle^{\mathrm{even}} = 8\tilde{\nu}\tilde{T}\tilde{R}^3 \tag{A.21n}$$

$$\left\langle (\hat{\boldsymbol{n}} \times \boldsymbol{v})^2 (\hat{\boldsymbol{n}} \times \boldsymbol{\Omega})^2 \right\rangle^{\mathrm{even}} = 0 \tag{A.21o}$$

$$\left\langle (\boldsymbol{v} \cdot \boldsymbol{\omega}) (\boldsymbol{V} \cdot \boldsymbol{\Omega}) \right\rangle^{\mathrm{odd}} = -20\tilde{\nu}\tilde{T}^2\tilde{R}^2 \tag{A.22a}$$

$$\left\langle (\hat{\boldsymbol{n}} \cdot \boldsymbol{v}) (\hat{\boldsymbol{n}} \cdot \boldsymbol{\omega}) (\boldsymbol{V} \cdot \boldsymbol{\Omega}) \right\rangle^{\mathrm{odd}} = -10\tilde{\nu}\tilde{T}^2\tilde{R}^2 \tag{A.22b}$$

$$\left\langle (\hat{\boldsymbol{n}} \cdot \boldsymbol{V}) (\hat{\boldsymbol{n}} \cdot \boldsymbol{\Omega}) (\boldsymbol{v} \cdot \boldsymbol{\omega}) \right\rangle^{\mathrm{odd}} = -7\tilde{\nu}\tilde{T}^2\tilde{R}^2 \tag{A.22c}$$

$$\left\langle (\hat{\boldsymbol{n}} \cdot \boldsymbol{v}) (\hat{\boldsymbol{n}} \cdot \boldsymbol{V}) (\hat{\boldsymbol{n}} \cdot \boldsymbol{\omega}) (\hat{\boldsymbol{n}} \cdot \boldsymbol{\Omega}) \right\rangle^{\mathrm{odd}} = -4\tilde{\nu}\tilde{T}^2\tilde{R}^2 \tag{A.22d}$$

$$\left\langle [(\hat{\boldsymbol{n}} \times \boldsymbol{v}) \cdot \boldsymbol{V}][(\hat{\boldsymbol{n}} \times \boldsymbol{\Omega}) \cdot \boldsymbol{\omega}] \right\rangle^{\mathrm{odd}} = 0 \tag{A.22e}$$

$$\left\langle (\hat{\boldsymbol{n}} \cdot \boldsymbol{\omega}) (\hat{\boldsymbol{n}} \cdot \boldsymbol{\Omega}) (\boldsymbol{v} \cdot \boldsymbol{V}) \right\rangle^{\mathrm{odd}} = -2\tilde{\nu}\tilde{T}^2\tilde{R}^2 \tag{A.22f}$$

$$\left\langle [(\hat{\boldsymbol{n}} \times \boldsymbol{v}) \cdot \boldsymbol{\omega}][(\hat{\boldsymbol{n}} \times \boldsymbol{\Omega}) \cdot \boldsymbol{V}] \right\rangle^{\mathrm{odd}} = -5\tilde{\nu}\tilde{T}^2\tilde{R}^2 \, . \tag{A.22g}$$

2. The correction terms for the temperatures

To calculate $dT/dt = \langle i\mathfrak{L}_+ T\rangle_t$ one essentially proceeds along the same lines of reasoning as detailed above. First of all, it is again advantageous to write the corrections to the Gaussian distribution function explicitly, that is,

$$\langle i\mathfrak{L}_+ T\rangle_t = \left\langle \left(\hat{b}_{12} - 1\right) T \right\rangle^{(0)} + b(t) \left\langle \left(\hat{b}_{12} - 1\right) T \right\rangle^{(1)} \tag{A.23}$$

where

$$\begin{aligned} \frac{3}{4m} \left(\hat{b}_{12} - 1\right) T = {} & \eta_t (\eta_t - 1) (\hat{\boldsymbol{n}} \times \boldsymbol{v})^2 \\ & + \eta_n (\eta_n - 1) (\hat{\boldsymbol{n}} \cdot \boldsymbol{v})^2 \\ & + \eta_t^2 a^2 (\hat{\boldsymbol{n}} \times \boldsymbol{\Omega})^2 \\ & + \eta_t (2\eta_t - 1)\, a \boldsymbol{v} \cdot (\hat{\boldsymbol{n}} \times \boldsymbol{\Omega}) \end{aligned} \tag{A.24}$$

and

$$\begin{aligned}\frac{3}{4m}\left(\hat{b}_{12}-1\right)R &= \frac{\eta_t^2}{q}\left(\hat{\boldsymbol{n}}\times\boldsymbol{v}\right)^2\\ &+ \eta_t\left(\frac{\eta_t}{q}+1\right)a^2\left(\hat{\boldsymbol{n}}\times\boldsymbol{\Omega}\right)^2 \qquad \text{(A.25)}\\ &+ \eta_t\left(\frac{2\eta_t}{q}+1\right)a\boldsymbol{v}\cdot\left(\hat{\boldsymbol{n}}\times\boldsymbol{\Omega}\right)\,.\end{aligned}$$

The term $\left\langle\left(\hat{b}_{12}-1\right)T\right\rangle^{(0)}$ is already known [25] and the only other contribution is $\left\langle\left(\hat{\boldsymbol{n}}\times\boldsymbol{\Omega}\right)^2\right\rangle^{\text{even}} = 2\tilde{\nu}\tilde{T}\tilde{R}^2$.

---

[1] I. Goldhirsch, Ann. Rev. Fluid Mech. **35**, 267 (2003).

[2] A. Levy and H. Kalman, *Handbook of Conveying and Handling of Particulate Solids* (Elsevier, Amsterdam, 2001).

[3] R. Greenberg and A. Brahic, eds., *Planetary Rings* (Arizona Univ. Press., Tucson, 1984).

[4] T. Pöschel and S. Luding, eds., *Granular Gases*, vol. 564 of *Lecture Notes in Physics* (Springer, Berlin, 2001).

[5] T. Pöschel and N. V. Brilliantov, eds., *Granular Gas Dynamics*, vol. 624 of *Lecture Notes in Physics* (Springer, Berlin, 2003).

[6] N. V. Brilliantov and T. Pöschel, *Kinetic Theory of Granular Gases* (Oxford University Press, Oxford, 2004).

[7] S. McNamara and W. R. Young, Phys. Fluids A **4**, 496 (1992).

[8] I. Goldhirsch and G. Zanetti, Phys. Rev. Lett. **70**, 1619 (1993).

[9] R. Brito and M. H. Ernst, Europhys. Lett. **43**, 497 (1998).

[10] A. Goldshtein and M. Shapiro, J. Fluid Mech. **282**, 75 (1995).

[11] T. P. C. van Noije and M. H. Ernst, Granular Matter **1**, 57 (1998).

[12] S. E. Esipov and T. Pöschel, J. Stat. Phys. **86**, 1385 (1997).

[13] J. J. Brey, D. Cubero, and M. J. Ruiz-Montero, Phys. Rev. E **59**, 1256 (1999).

[14] P. Deltour and J.-L. Barrat, J. Physique I **7**, 137 (1997).

[15] M. Huthmann, J. Orza, and R. Brito, Granular Matter **2**, 189 (2000).

[16] N. V. Brilliantov and T. Pöschel, Phys. Rev. E **61**, 2809 (2000).

[17] I. Goldhirsch, H. S. Noskowicz, and O. Bar-Lev, in [5], pp. 37–63.

[18] T. Pöschel, N. V. Brilliantov, and A. Formella, Phys. Rev. E **74**, 041302 (2006).

[19] J. J. Brey, M. J. Ruiz-Montero, and R. Garcia-Rojo, Phys. Rev. E **60**, 7174 (1999).

[20] J. J. Brey, M. J. Ruiz-Montero, D. Cubero, and R. Garcia-Rojo, Physics of Fluids **12**, 876 (2000).

[21] N. V. Brilliantov and T. Pöschel, Phys. Rev. E **61**, 1716 (2000).

[22] A. Santos and J. W. Dufty, Phys. Rev. Lett. **86**, 4823 (2001).

[23] V. Garzo and J. M. Montanero, Phys. Rev. E **69**, 021301 (2004).

[24] M. Huthmann and A. Zippelius, Phys. Rev. E **56**, R6275 (1997).

[25] T. Aspelmeier, M. Huthmann, and A. Zippelius, in [4], p. 31.

[26] I. Goldhirsch, S. H. Noskowicz, and O. Bar-Lev, J. Phys. Chem. **109**, 21449 (2005).

[27] T. Elperin and E. Golshtein, Physica A **247**, 67 (1997).

[28] J. T. Jenkins and M. W. Richman, Physics of Fluids **28**, 3485 (1985).

[29] C. K. K. Lun and S. B. Savage, J. Appl. Mech. Trans. ASME **54**, 47 (1987).

[30] H. M. Jaeger, C. Liu, S. R. Nagel, and T. A. Witten, Europhys. Lett. **11**, 619 (1990).

[31] S. Luding, Phys. Rev. E **52**, 3416 (1995).

[32] J. T. Jenkins and M. Louge, Physics of Fluids **9 (10)**, 2835 (1997).

[33] S. G. Bardenhagen, J. U. Brackbill, and D. Sulsky, Phys. Rev. E **62**, 3882 (2000).

[34] R. Cafiero, S. Luding, and H. J. Herrmann, Europhys. Lett. **60**, 854 (2002).

[35] N. Mitarai, H. Hayakawa, and H. Nakanishi, Phys. Rev. Lett. **88**, 174301 (2002).

[36] I. Goldhirsch, S. H. Noskowicz, and O. Bar-Lev, Phys. Rev. Lett. **95**, 068002 (2005).

[37] N. V. Brilliantov, T. Pöschel, W. T. Kranz, and A. Zippelius, Phys. Rev. Lett. **98**, 128001 (2007).

[38] N. V. Brilliantov, F. Spahn, J.-M. Hertzsch, and T. Pöschel, Phys. Rev. E **53**, 5382 (1996).

[39] T. Schwager and T. Pöschel, Phys. Rev. E **57**, 650 (1998).

[40] R. Ramírez, N. V. Brilliantov, T. Schwager, and T. Pöschel, Phys. Rev. E **60**, 4465 (1999).

[41] V. Becker, T. Schwager, and T. Pöschel, Phys. Rev. E **77**, 011304 (2008).

[42] S. Luding, M. Huthmann, S. McNamara, and A. Zippelius, Phys. Rev. E **58**, 3416 (1998).

[43] T. Pöschel, N. V. Brilliantov, and T. Schwager, Int. J. Mod. Phys. C **13**, 1263 (2003).

[44] S. H. Noskowicz, O. Bar-Lev, D. Serero, and I. Goldhirsch, Europhys. Lett. **79**, 60001 (2007).

[45] G. A. Bird, *Molecular Gas Dynamics and the Direct Simulation of Gas Flows* (Oxford University Press, 1994).

[46] T. Pöschel and T. Schwager, *Computational Granular Dynamics* (Springer, New York, 2005).

[47] B. Gayen and M. Alam, Phys. Rev. Lett. **1**, 068002 (2008).

[48] J. J. Brey and D. Cubero, in *Granular Gases*, edited by T. Pöschel and S. Luding (Springer, Berlin, 2001), vol. 564 of *Lecture Notes in Physics*, p. 59.

[49] To be precise, although the mathematical operations in DSMC looks like a particle simulation, the particles in the simulation do not correspond to real particles. They are better considered as quanta of probability [48].